Proceedings of the 5th International Conference on Fluid Flow and Thermal Science (ICFFTS 2024)
Lisbon, Portugal- November 21 - 23, 2024
Paper No. 158
DOI: 10.11159/icffts24.158

Optimal Heat Transfer Coefficients for Sustained PCM Functionality in High-Rate Discharge Cycle of Lithium-Ion Battery

Vanita A. Wagh[1], Sandip K. Saha[1]
[1]Indian Institute of Technology Bombay
Powai, Mumbai-400076, India
214100027@iitb.ac.in; sandip.saha@iitb.ac.in

Abstract - Lithium-ion batteries (LIBs) are crucial for electric vehicles (EVs) due to their high energy storage capacity. Effective thermal management is vital, as these batteries need to operate within an optimal temperature range of 15 to 45 °C to ensure longevity and prevent thermal runaway. This study focuses on determining the optimal heat transfer coefficient (*h*) required to facilitate the full melting of phase change materials (PCMs) during high-rate discharging and to ensure their complete solidification during the subsequent charging phase for effective and continuous use of PCM. The analysis addresses the thermal management requirements necessary to sustain phase stability and efficient heat exchange across repeated high-frequency discharging-charging cycles. Utilizing the Newman-Tiedemann-Gu-Kim (NTGK) model, the research simulates the performance of the SAMSUNG ICR 18650-26J Lithium-ion battery. The cell is encased by a copper shell, followed by the addition of the PCM, and then further encapsulated by another copper shell. The NTGK model's effectiveness is validated through simulations, demonstrating its accuracy in predicting thermal behaviours across different conditions. The present study evaluated three PCMs such as n-Heneicosane, OM42, and n-Docosane and a range of heat transfer coefficients (*h*) from 20 W/m²·K to 500 W/m²·K for the thermal management of cells. It is found that increasing the PCM thickness from 3 mm to 4 mm reduces the maximum cell temperature from 53.19 °C to 51.94 °C during a 5C discharge at 40 °C ambient temperature, however, resulting in lower PCM utilization, making 3 mm as the optimal PCM thickness. At an ambient temperature of 35 °C, n-Heneicosane remains in the liquid state, whereas n-Docosane maintained better thermal regulation and complete solidification, demonstrating its suitability for moderate ambient conditions. Under harsh conditions (40°C), increasing the convective heat transfer coefficient to 500 W/m²·K during charging allows n-Docosane to solidify within 750 s fully, ensuring effective thermal management. This research provides essential insights for optimizing thermal management systems in LIBs for EVs, enhancing performance and safety.

***Keywords*:** Lithium-ion batteries, phase change materials, NTGK model, discharging-charging cycles

1. Introduction

Road transportation is a significant contributor to global greenhouse gas emissions, accounting for about 72% of the transportation sector's emissions [1]. In some regions, it is responsible for 85.2% of CO_2 emissions [2]. Emissions from conventional road transport not only increase greenhouse gases but also deteriorate air quality, particularly in urban areas, through pollutants like CO_2, sulfur dioxide (SO_2), and nitrogen oxides (NO_x) [3]. The urgent need to address environmental concerns, particularly greenhouse gas emissions and air pollution, has shifted research priorities towards greener alternatives such as battery electric vehicles (EVs). Factors influencing the diffusion of EVs in urban areas are being studied intensively [1], emphasizing the importance of transitioning to cleaner transportation options to address environmental challenges effectively.

Lithium-ion batteries have seen significant advancements, enhancing their adaptability in electric vehicles (EVs) and other applications. Key improvements include the development of high-capacity cathode materials, which increase energy density for EV use [2]. Research has also focused on integrating lithium-ion batteries with technologies like perovskite solar cells to enhance performance and charging capabilities [3]. Lithium-ion batteries' high specific power, specific energy, long lifespan, and compact size and weight make them suitable for the high-energy storage demands of EVs. Additionally, the development of lithium-free transition metal monoxides for positive electrodes has improved energy/power density, reduced costs, and extended cycle life, which is critical for EVs and large-scale energy storage [4].

In addressing thermal management challenges in battery systems, phase change materials (PCMs) have been increasingly incorporated into Battery Thermal Management Systems (BTMS). These advantages of using PCMs include enhanced thermal regulation, improved energy efficiency, and reduced system complexity. By utilizing PCMs in BTMS, the heat generated during battery operation is absorbed by the PCM as it changes its phase from solid to liquid, effectively storing and dissipating heat. This process helps to maintain the battery temperature within a safe operating range, preventing overheating and ensuring optimal performance. Karmkar et al. [5] discussed how PCMs have high latent heat capacities, allowing them to absorb and release large amounts of energy during phase transitions and efficiently manage thermal fluctuations in battery systems. Song et al. [6] demonstrated that compared to traditional cooling methods, PCMs offer passive thermal management, eliminating the need for active cooling components like fans or pumps, which can consume additional energy and add complexity to the system. Zhang et al. [7] highlighted that PCMs provide more uniform temperature distribution within the battery pack, reducing hotspots and enhancing overall system reliability. In conclusion, integrating phase change materials into battery thermal management systems offers a sustainable and effective solution to address thermal challenges, providing efficient heat dissipation, improved energy efficiency, and enhanced system reliability compared to traditional cooling methods.

The thermal management of lithium-ion batteries encased with PCMs is crucial for their performance and safety during high-rate discharging and charging cycles. A higher heat transfer coefficient aids in efficient heat dissipation, managing the heat generated during rapid charging and discharging processes. This allows for quick heat transfer to the PCM, enabling effective absorption and storage of excess heat, thus maintaining the battery temperature within a safe operating range. Wagh et al. [8] found that incorporating fins in the PCM can enhance heat dissipation capacity by improving heat transfer. Li et al. [9] discussed using different PCMs, such as RT15, RT31, EG5, and EG26, which have been experimentally investigated to enhance heat transfer rates and the overall thermal performance of electric vehicle battery packs. Angani et al. [10] highlighted that integrating PCMs in battery packs has demonstrated improved heat transfer rates and thermal performance under extreme temperature conditions, contributing to better thermal regulation and safety of the battery system. Talluri et al. [11] also supported these findings by showing the benefits of PCMs in maintaining optimal battery temperatures. However, despite these advancements, a significant research gap remains in understanding the specific heat transfer coefficients required for the complete solidification of PCMs during continuous high-rate discharging-charging cycles.

While various PCMs have been studied, n-Heneicosane, OM42, and n-Docosane are selected for this study due to their specific melting temperatures (43.6 °C, 43 °C, and 44.7 °C, respectively), which closely align with India's ambient temperature conditions. This makes them particularly suitable for thermal management in environments with similar climatic characteristics. This research evaluates these PCMs in managing the thermal behaviour of SAMSUNG ICR 18650-26J Lithium-ion battery, focusing on maintaining battery temperatures within the crucial range of 15 °C to 45 °C during high-rate discharging and charging cycles [12]. This study systematically analyzes the high discharge rate (5C) configuration combined with charging rates (1C), providing comprehensive insights into their thermal behaviour. This study investigates heat transfer coefficients from 20 $W/m^2 \cdot K$ to 500 $W/m^2 \cdot K$ to determine optimal values for maintaining safe battery temperatures and necessary for effective PCM solidification during continuous high-rate cycles for harsh ambient conditions. By examining specific PCMs and heat transfer coefficients, the study aims to enhance battery safety and performance under high C-rate cycles. The findings provide new insights into the critical heat transfer coefficients for PCM solidification, offering valuable data on PCM effectiveness in specific configurations.

2. Methodology

2.1. Battery and PCM Selection with Numerical Analysis Setup

The study utilizes a SAMSUNG ICR 18650-26J Lithium-ion battery with a nominal capacity of 2600 mAh. The battery has an 18 mm diameter core, encased within a 0.5 mm thick inner copper shell, surrounded by a 3 mm layer of PCM, and further encapsulated by a 0.5 mm outer copper shell, with 1 mm thick caps on both the top and bottom. The selected PCMs, n-Heneicosane, OM42, and n-Docosane, are chosen for their melting points and thermal properties, optimal for maintaining

battery temperature during high-rate discharging and charging cycle of 5C-1C configuration. The performance of battery-PCM configuration is examined under heat transfer coefficients ranging from 20 to 500 W/m²·K. The specifications and properties of the battery can be found in [13]. The thermophysical properties of PCMs are listed in Table 1.

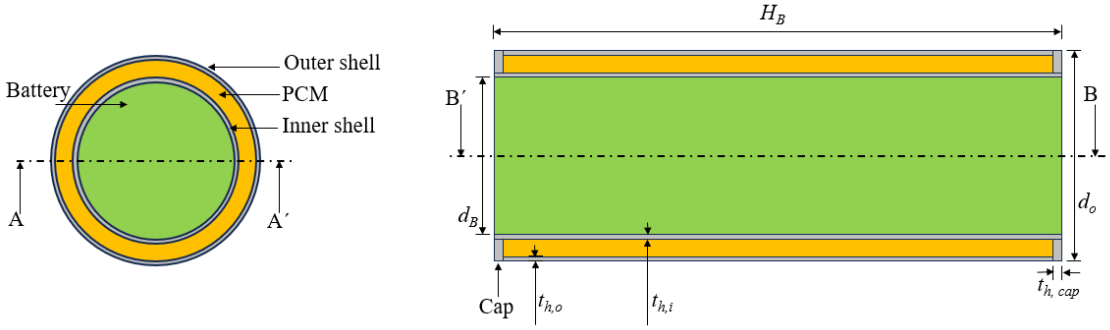

Fig. 1: Battery encased with copper shells and PCM.

Table 1: Thermophysical properties of n-Docosane [14], n-Heneicosane and OM42

Property	n-Docosane	n-Heneicosane	OM42
Density (kg/m³)	778	772	865
Reference temperature (°C)	42.1	39.2	43
Volumetric thermal expansion coefficient (K^{-1})	1×10^{-3}	1×10^{-3}	1×10^{-3}
Thermal conductivity (W/m·K)	0.21	0.145	0.19
Melting point (°C)	44.7	43.6	43
Latent heat of fusion (J/kg)	257000	294600	183000
Specific heat capacity (J/kg·K)	2650	2386	2710
Dynamic viscosity (kg/m·s)	0.003933	0.0032793	0.0038925

2.2. Numerical Model and Simulation

The thermal performance of the battery is simulated using the Newman-Tiedemann-Gu-Kim (NTGK) model. The governing equations for the thermal and electrical energy conservation within the battery are solved using a Multi-Scale Multi-Domain (MSMD) approach [8]. The governing equations for current flux at both the positive and negative electrodes are detailed as [15], [16].

$$\frac{\partial\left(\rho_B c_B T_B\right)}{\partial t} = \nabla\cdot\left(K_B\nabla T_B\right) + \sigma_+|\nabla\phi_+|^2 + \sigma_-|\nabla\phi_-|^2 + \dot{q}_{ECh} + \dot{q}_{short} \tag{1}$$

$$\nabla\cdot\left(\sigma_+\nabla\phi_+\right) = -\left(j_{ECh} - j_{short}\right) \tag{2}$$

$$\nabla\cdot\left(\sigma_-\nabla\phi_-\right) = \left(j_{ECh} - j_{short}\right) \tag{3}$$

The enthalpy method is employed to model the solidification and melting of the PCM. The fluid flow of the PCM is assumed to be laminar and Newtonian, with constant property values across the temperature range considered in the study. The governing equations that describe the PCM domain are presented below:

Conservation of Mass:

$$\frac{\partial\rho_p}{\partial t} + \nabla.\left(\rho_p\vec{V}\right) = 0 \tag{4}$$

Conservation of Momentum:

$$\left(\frac{\partial}{\partial t} + \nabla.\vec{V}\right)\left(\rho_p\vec{V}\right) = -\nabla P + \nabla.\left(\mu\nabla\vec{V}\right) + S_u + \frac{\rho_p g\beta\left(e - e_{ref}\right)}{c_p} \tag{5}$$

Conservation of Energy:

$$\frac{\partial\left(\rho_p c_p T\right)}{\partial t} + \nabla.\left(\rho_p\vec{V}c_p T\right) = \nabla.\left(K_p\nabla T\right) + S_h \tag{6}$$

where the velocity vector, $\vec{V} = u\hat{i} + v\hat{j} + w\hat{k}$. The source term S_u is used to model fluid flow during phase change. β is a thermal expansion coefficient and e_{ref} is a reference value of the sensible heat. S_h is a phase related source term. The liquid fraction of PCM is expressed as,

$$f_l = \frac{\Delta E}{L} \tag{7}$$

The initial temperature of the battery and PCM is set to the ambient temperature of 40 °C. The PCM is initially in a solid phase, and the velocity field is set to zero.

$$\text{At } t = 0;\ T(x,y,z) = T_a = 40\ ^\circ C \text{ and } \vec{V} = 0, \tag{8}$$

Based on Newton's law of cooling, the boundary condition on the external housing surface is given as:

$$k_{cu}\frac{\partial T_{cu,o}}{\partial r} = h(T_{cu,o} - T_a) \tag{9}$$

The numerical analysis is conducted using the finite volume-based ANSYS Fluent 2021/R2 commercial solver. The Pressure-Implicit with Splitting of Operators (PISO) algorithm is used to couple pressure and velocity. The PRESTO! scheme is applied for the discretization of the pressure equation, while a second-order upwind scheme is used for the discretization of momentum and energy equations.

The present numerical model is based on the NTGK model and is validated against the experimental study by Trimbake et al. [17] and the numerical analysis by Jithin et al. [13]. Both studies investigate a Samsung 26J 18650 2600 mAh battery pack in a 4S1P configuration. The experiments discharged the batteries at 2C (5.2A) and 1C (2.6A) using a 200 W electronic load, focusing on a 1C discharge scenario with h= 5 W/m²·K. Fig. 2 compares the battery's cell temperature over time using experimental and numerical data.

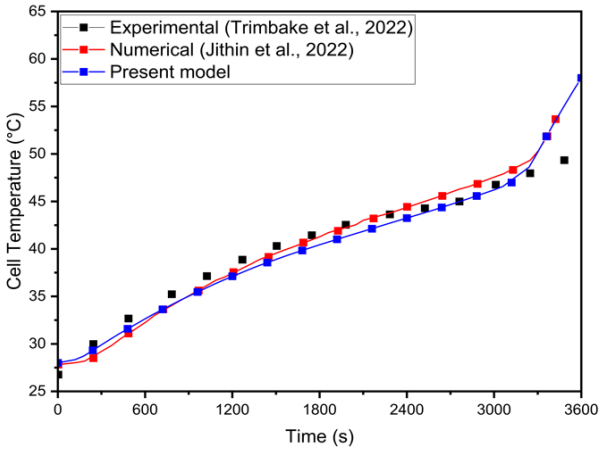

Fig. 2. Model validation of battery pack with experimental results [17], and numerical results [8], [13]

Temperature measurements revealed a distinct pattern: a rapid initial rise, a gradual increase, and a final spike, which is accurately predicted by the present numerical model. The numerical results closely match the experimental data, with maximum deviations of 11.48% and 2.95% compared to Trimbake et al. [17] and Jithin et al. [13], respectively.

3. Results and Discussion

3.1 Effect of PCM Thickness

In thermal management systems for lithium-ion batteries, selecting the optimal thickness of PCMs is crucial to balance temperature control and material efficiency. Fig. 3 presents the temperature profiles for both the cell and the PCM during a 5C discharging cycle at an ambient temperature of 40 °C, comparing PCM thicknesses of 3 mm and 4 mm. The materials analyzed are n-Heneicosane, OM42, and n-Docosane, with h=20 W/m²·K. The results in Fig. 3(a) reveal that the maximum cell temperatures at the end of the discharging cycle reach 53.19 °C, 55.31 °C, and 52.23 °C for the 3 mm thick layers of n-Heneicosane, OM42, and n-Docosane, respectively. When the PCM thickness is increased to 4 mm, the maximum cell temperatures are slightly reduced to 51.94 °C, 53.16 °C, and 51.55 °C for the respective materials. This reduction indicates

that thicker PCM layers absorb more heat during the high-rate discharging cycle, thus keeping the cell temperature within the target operational range. Similarly, the maximum PCM temperatures, as seen in Fig. 3(a), reach 47.13 °C, 50.72 °C, and 46.20 °C for the 3 mm thick layers of n-Heneicosane, OM42, and n-Docosane, respectively. With 4 mm thick PCM layers, these temperatures decrease to 43.92 °C, 45.57 °C, and 44.67 °C, respectively. Fig. 3(b) shows the liquid fraction of the PCMs over time, highlighting the extent of melting during the discharging cycle. For the 3 mm thick PCMs, the maximum melting fractions are 98.01%, 100%, and 93.04% for n-Heneicosane, OM42, and n-Docosane, respectively. In contrast, the 4 mm thick PCMs show significantly lower melting fractions of 43.92%, 45.57%, and 44.67%. This suggests that thicker PCM layers are more effective at temperature control, however do not fully utilize their latent heat capacity during the cycle. Considering the balance between temperature regulation and effective material utilization, the 3 mm PCM thickness emerges as the optimal choice across all three materials.

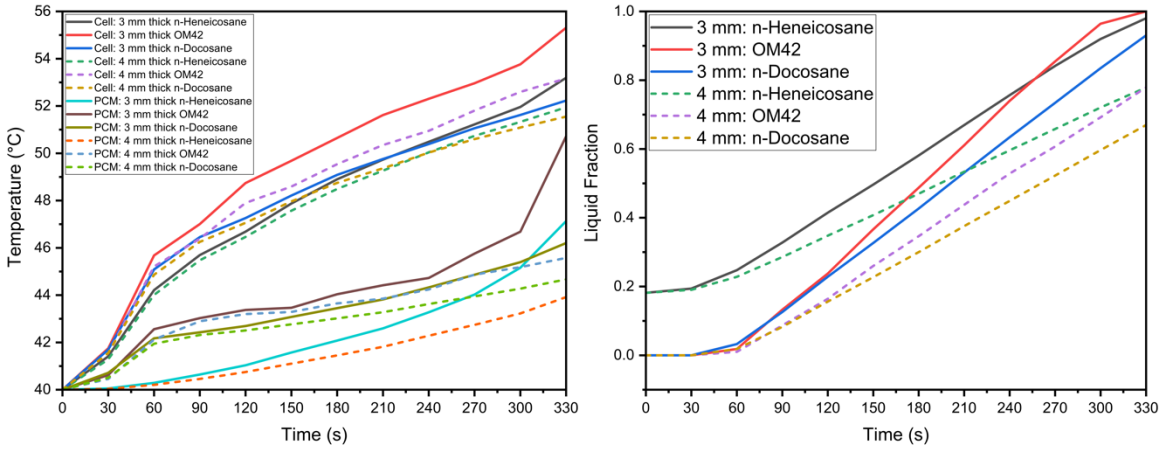

Fig. 3. Effect of PCM thickness on thermal management during a 5C discharging cycle at 40°C ambient temperature and h=20 W/m²·K, (a) Cell and PCM temperature profiles. (b) Liquid fraction profiles.

3.2 Effect of ambient temperatures on PCM with cell

The performance of PCMs in managing the thermal behaviour of LIBs is highly sensitive to changes in ambient temperature. Fig. 4 presents the effect of ambient temperature on the thermal management performance of n-Heneicosane, OM42, and n-Docosane during a 5C discharging cycle, with a PCM thickness of 3 mm and h=20 W/m²·K. In Fig. 4(a), the cell temperature profiles indicate that as the ambient temperature increases from 30 °C to 40 °C, the maximum cell temperature rises correspondingly for all PCMs. OM42 results in the highest cell temperatures across all ambient conditions, suggesting that while it effectively melts and absorbs heat, its capacity to maintain lower cell temperatures diminishes as the ambient temperature rises. Fig. 4(b) shows the corresponding PCM temperature profiles. The maximum PCM temperature also increases with rising ambient temperatures. OM42 exhibits the highest temperature rise, indicating a more significant phase change, which aligns with its higher melting fraction and the corresponding cell temperature results. Fig. 4(c) illustrates the liquid fraction of the PCMs, highlighting the extent of melting under different ambient conditions. The maximum melting fraction reaches 57.41%, 72.02%, and 98.01% for n-Heneicosane; 67.13%, 88.09%, and 100% for OM42; and 58.73%, 75.70%, and 93.04% for n-Docosane at ambient temperatures of 30 °C, 35 °C, and 40 °C, respectively. As expected, higher ambient temperatures lead to greater PCM melting, with OM42 achieving complete melting at 40 °C, which correlates with its higher cell and PCM temperatures observed earlier. Among the PCMs tested, n-Docosane demonstrates the most consistent performance across the different ambient temperatures, maintaining lower cell and PCM temperatures under the most extreme conditions.

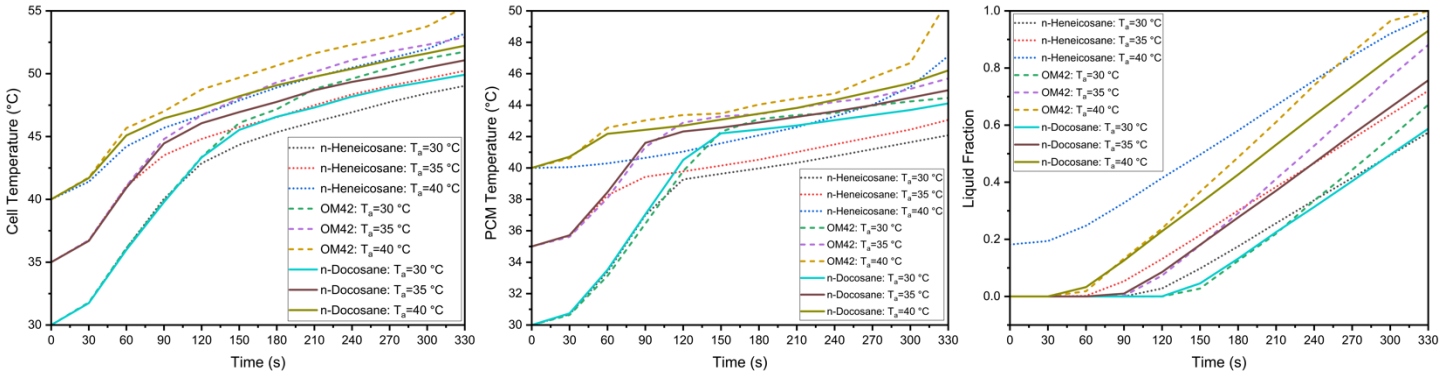

(a) (b) (c)

Fig. 4. Effect of ambient temperatures on thermal management with 3 mm PCM thickness and h=20 W/m²·K, (a) Cell temperature profiles, (b) PCM temperature profiles, (c) Liquid fraction of PCMs

3.3 PCMs Thermal Performance at 35 °C

This study focuses on the thermal behaviour of PCMs near their melting points, specifically focusing on 35 °C, an ambient temperature common during summer in India. Fig. 5 illustrates the thermal behaviour of n-Heneicosane, OM42, and n-Docosane during a 5C discharging cycle followed by a 1C charging cycle at an ambient temperature of 35 °C, with a PCM thickness of 3 mm and h=20 W/m²·K during discharging, and h=50 and 100 W/m²·K during charging.

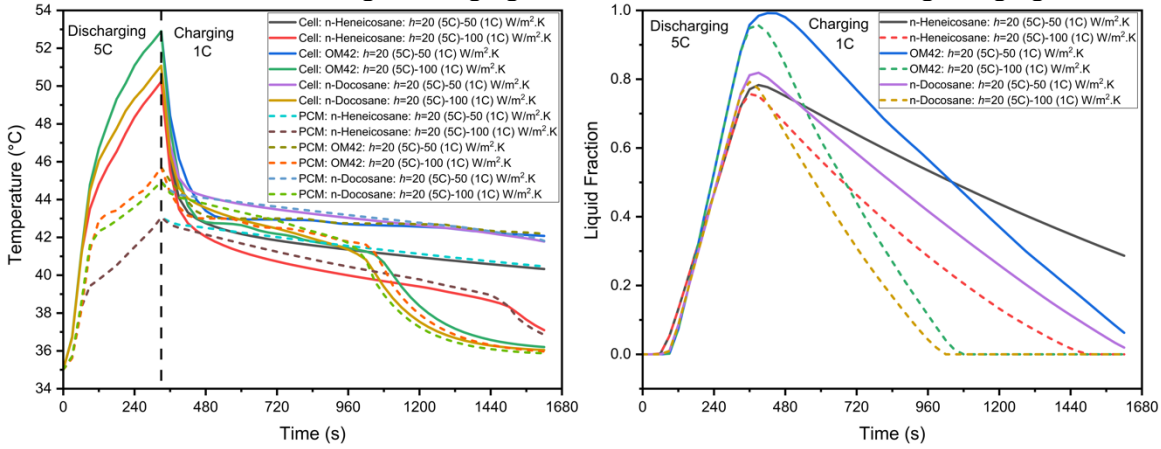

(a) (b)

Fig. 5. Temperature and liquid fraction profiles during a 5C discharging and 1C charging cycle with 3 mm PCM thickness and h=20 W/m²·K for discharging and h=50 and 100 W/m²·K for charging, (a) Cell and PCM temperature profiles, (b) Liquid fraction of PCMs.

Fig. 5(a) shows that the maximum cell temperatures during the 5C discharging cycle reach 50.23°C, 52.90°C, and 51.07°C for n-Heneicosane, OM42, and n-Docosane, respectively. The corresponding maximum PCM temperatures, as depicted in Fig. 5(a), are 43.06°C, 45.7°C, and 44.95°C. Among these, OM42 exhibits the highest temperature rise, indicating a more significant phase change and greater heat absorption than other PCMs. Fig. 5(b) reveals the liquid fraction profiles at the end of the discharging cycle, where the maximum melting percentages are 72.02%, 88.09%, and 75.70% for n-Heneicosane, OM42, and n-Docosane, respectively. During the subsequent 1C charging process, the initial heat transfer coefficient of h=50 W/m²·K proves inadequate for complete PCM solidification by the end of the cycle, leaving temperatures elevated. Thus, a higher coefficient of h=100 W/m²·K results in a sudden drop in temperature as the PCMs fully solidify at

approximately 1200 s, 780 s, and 720 s for n-Heneicosane, OM42 and n-Docosane, respectively. This rapid solidification underscores the effectiveness of a higher heat transfer coefficient in hastening the thermal recovery of the PCM. It can be concluded that n-Docosane emerges as the optimum PCM for ensuring both effective heat management and rapid thermal recovery in lithium-ion battery systems operating under these conditions.

3.4 Solidification at Harsh Conditions (40 °C, n-Docosane)

This section examines n-Docosane's solidification efficiency under extreme conditions at 40 °C, which is critical for maintaining battery performance during rapid cycles. Fig. 6 illustrates the thermal behaviour and phase change characteristics of n-Docosane during a 5C discharging cycle followed by a 1C charging cycle under harsh ambient conditions of 40 °C. Fig. 6(a) shows that the maximum cell temperature reaches 52.23 °C, while the maximum PCM temperature reaches 46.20 °C at the end of the 5C discharging cycle. The melt fraction of n-Docosane is 93.04%, as shown in Fig. 6(b). Following the discharging phase, the 1C charging process begins, and Fig. 6(a) demonstrates the usefulness of a higher heat transfer coefficient in achieving complete solidification. At h=50 and 100 W/m²·K, the PCM does not fully solidify at the end of the charging cycle, as indicated by the higher temperatures and liquid fraction seen in Fig. 6(b). Consequently, higher heat transfer coefficients of h=200 and 500 W/m²·K are applied, resulting in rapid temperature decrease and complete solidification of n-Docosane. The time required for solidification is significantly reduced, with h=200 W/m²·K achieving solidification in 1290 s and h=500 W/m²·K in 750 s.

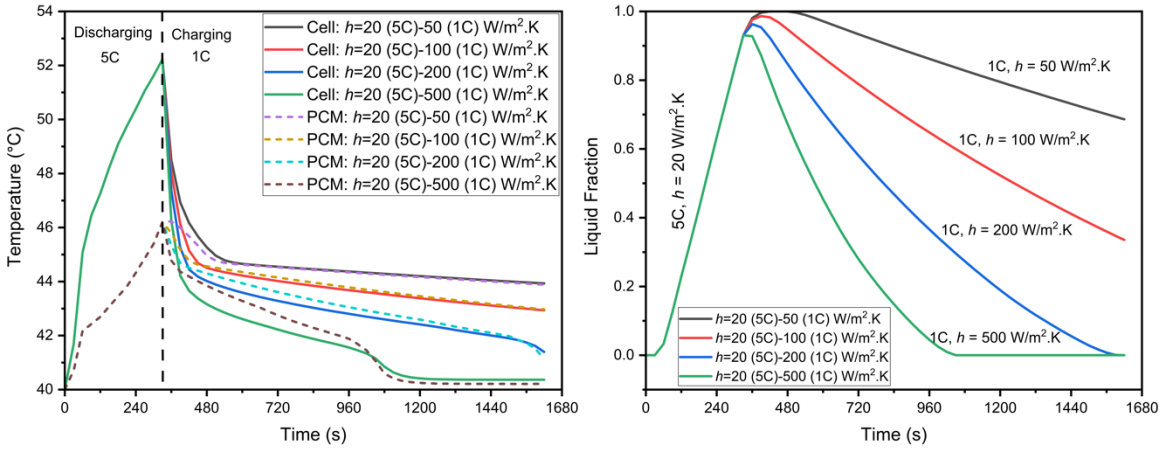

Fig. 6. (a) Cell and PCM temperature, (b) liquid fraction, profiles during a 5C discharging and 1C charging cycle with 3 mm n-Docosane and h=20 W/m²·K for discharging and various heat transfer coefficients for charging.

This outcome demonstrates the importance of optimizing convective heat transfer in maintaining effective thermal management under extreme conditions.

4. Conclusion

This study investigated the thermal management of lithium-ion batteries using PCMs under different conditions, focusing on PCM thickness, ambient temperature, and convective heat transfer coefficients. The objective is to determine the optimal PCM configuration for maintaining safe battery temperatures during high-rate discharging and charging cycles, particularly under challenging conditions. Increasing the PCM thickness from 3 mm to 4 mm results in lower maximum cell temperatures. However, the 4 mm thickness shows reduced PCM utilization, making 3 mm the optimal thickness for balancing temperature control and PCM efficiency. Ambient temperatures between 30 °C and 40 °C directly affect PCM and cell temperatures. The highest cell temperature observed for OM42 at 40 °C is 55.31 °C, indicating a decreased heat transfer performance with rising ambient temperatures despite complete PCM melting. In contrast, n-Docosane demonstrated superior thermal regulation and complete solidification, making it more suitable for these conditions. At a typical ambient

temperature of 35 °C in India, n-Docosane maintained lower peak temperatures and solidified more efficiently during charging. Under extreme conditions of 40 °C, n-Docosane requires increased convective heat transfer coefficients to achieve complete solidification during the charging cycle. At a coefficient of 500 W/m²·K, the solidification of PCM is completed within 750 s, highlighting the importance of enhanced cooling for maintaining battery performance. This study identified n-Docosane as the most effective PCM for lithium-ion battery thermal management across various conditions, providing reliable temperature regulation and efficient phase transitions.

References

[1] M. Mashayekhi, "Factors Influencing the Diffusion of Battery Electric Vehicles in Urban Areas," Ryerson University Library and Archives, Jun. 2021.

[2] P. K. Nayak, E. M. Erickson, F. Schipper, T. R. Penki, N. Munichandraiah, P. Adelhelm, H. Sclar, F. Amalraj, B. Markovsky and D. Aurbach, "Review on Challenges and Recent Advances in the Electrochemical Performance of High Capacity Li and MnRich Cathode Materials for LiIon Batteries," *Adv. Energy Mater.*, vol. 8, no. 8, Dec. 2017.

[3] J. Xu, Y. Chen, and L. Dai, "Efficiently photo-charging lithium-ion battery by perovskite solar cell," *Nat. Commun.*, vol. 6, no. 1, Aug. 2015.

[4] S. K. Jung, H. Kim, M. G. Cho, S. P. Cho, B. Lee, H. Kim, Y. U. Park, J. Hong, K. Y. Park, G. Yoon, W. M. Seong, Y. Cho, M. H. Oh, H. Kim, H. Gwon, I. Hwang, T. Hyeong, W. S. Yoon and K. Kang, "Lithium-free transition metal monoxides for positive electrodes in lithium-ion batteries," *Nat. Energy*, vol. 2, no. 2, Jan. 2017.

[5] B. Karmkar, R. Mokal, S. Landge, and B. Jadhav, "Design and Implement a BTMS using Phase Change Material - A Review," *Int. J. Res. Appl. Sci. Eng. Technol.*, vol. 12, no. 5, pp. 4249–4253, May 2024.

[6] L. Song, "Thermal Performance Analysis of the Battery Thermal Management Using Phase Change Material," *OALib*, vol. 05, no. 12, pp. 1–5, 2018.

[7] C. W. Zhang, S. R. Chen, H. B. Gao, K. J. Xu, Z. Xia, and S. T. Li, "Study of Thermal Management System Using Composite Phase Change Materials and Thermoelectric Cooling Sheet for Power Battery Pack," *Energies*, vol. 12, no. 10, p. 1937, May 2019.

[8] V. A. Wagh and S. K. Saha, "Optimising extended fin design and heat transfer coefficient for improved heat transfer and PCM recover time in thermal management of batteries," *Appl. Therm. Eng.*, vol. 255, p. 123964, Oct. 2024, doi: 10.1016/j.applthermaleng.2024.123964.

[9] S. Li, Y. Cheng, Q. Shen, C. Wang, C. Peng, and G. Yang, "Numerical analysis on the thermal management of phase change material with fins for lithium-ion batteries," *Int. J. Numer. Methods Heat Amp Fluid Flow*, vol. 34, no. 3, pp. 1170–1188, Dec. 2023.

[10] A. Angani, E. Kim, and K. Shin, "Improvement of Thermal Performance of Electric Vehicle Battery Pack with Phase-change Material," *Sens. Mater.*, vol. 32, no. 5, p. 1609, May 2020.

[11] T. Talluri, T. H. Kim, and K. J. Shin, "Analysis of a Battery Pack with a Phase Change Material for the Extreme Temperature Conditions of an Electrical Vehicle," *Energies*, vol. 13, no. 3, p. 507, Jan. 2020.

[12] "Sony: Lithium Ion Rechargeable Batteries (Wayback Machine)." [Online]. Available: https://web.archive.org/web/20090411024100/http://www.sony.com.cn/products/ed/battery/download.pdf

[13] K. V. Jithin and P. K. Rajesh, "Numerical analysis of single-phase liquid immersion cooling for lithium-ion battery thermal management using different dielectric fluids," *Int. J. Heat Mass Transf.*, vol. 188, p. 122608, Jun. 2022, doi: 10.1016/j.ijheatmasstransfer.2022.122608.

[14] D. Velliadou, K. D. Antoniadis, A. N. Assimopoulou, M. J. Assael, M. C. M. Sequeira, and W. A. Wakeham, "Accurate Measurements of the Thermal Conductivity of n-Docosane, n-Tetracosane, 1,6-Hexanediol, and 1,8-Octanediol in the Solid and Liquid Phases," *Int. J. Thermophys.*, vol. 44, no. 5, Apr. 2023, doi: 10.1007/s10765-023-03182-6.

[15] A. N. S. Y. S. Inc, "ANSYS fluent theory guide." 2020. [Online]. Available: https://www.ansys.com

[16] M. S. Patil, J. H. Seo, and M. Y. Lee, "A novel dielectric fluid immersion cooling technology for Li-ion battery thermal management," *Energy Convers Manag*, vol. 229, 2021, doi: 10.1016/j.enconman.2020.113715.

[17] A. Trimbake, C. P. Singh, and S. Krishnan, “Mineral oil immersion cooling of lithiumion batteries: an experimental investigation,” *J Electrochem Energy Convers Storage*, vol. 19, no. 2, 2022, doi: 10.1115/1.4052094.